

Alignment control of liquid crystal molecules using crack induced self-assembled grooves

Tzu-Chieh Lin,* Li-Chen Huang, Tsu-Ruey Chou and Chih-Yu Chao*

Received 12th June 2009, Accepted 12th August 2009

First published as an Advance Article on the web 1st September 2009

DOI: 10.1039/b911567f

Molecule alignment has many significant applications in biotechnology, molecular electronics, optoelectronic devices and liquid crystal (LC) display manufacturing. In this paper, we employ a fast and high-throughput method, fabricating micro- and nano-grooves for the alignment of liquid crystal (LC) molecules. Splitting the polymer film sandwiched by two substrates triggers the propagating wave front to induce self-assembled grooves on the polymer surfaces. This crack-induced grooving (CIG) method not only avoids the high-temperature process, dust and ion contaminations caused by traditional rubbing, but also provides a large anchoring energy comparable to that using polyimide rubbing. This CIG method offers an appealing alternative to existing technologies for LC molecules alignment.

1. Introduction

Aligning LC molecules is a very important issue in manufacturing LC displays (LCD) and devices. It is well-understood that LC molecules would tend to orient along the direction of a groove due to the minimization of LC elastic energy on the groove surface.¹ Although traditionally polyimide (PI) rubbing is the most common technique for creating grooves on a polymer surface, and in turn renders LCs to align parallel to the groove's direction, it still has many intrinsic disadvantages like the high-temperature process (~ 250 °C), dust contamination, electrostatic problems, and many ions caused by rubbing. E-Beam lithography and AFM nano-rubbing were also utilized to tailor the polymer surface with nano-grooves for LC alignment, but the region of the pattern is very small and these techniques show a very low throughput.^{2,3} Besides that, nano-imprint lithography (NIL) and photolithography (PL) were employed to transfer grooves on polymer thin film for aligning LC molecules.^{4,5} However, both NIL and PL need a pre-fabricated mask and the period of the grooves is also limited.

In this paper, we propose a straightforward method, splitting a polymer film sandwiched by two substrates, for fabricating micro- or nano-grooves to align LC molecules. The scheme of this crack-induced grooving (CIG) method is shown in Fig. 1 which comprises several steps. In our experiment, strong adhesion between polymer and substrates is influential in forming grooves, but do not affect the period of grooves. As shown in Fig. 1(a), pressing and heating the sandwiched polymer between two substrates improves the adhesion. Pulling apart the two substrates applies a driving force which would create a sufficiently large tensile stress to trigger the crack. (Fig. 1 (b)) When the crack edge approaches the stiff surface of the substrate, it would be reflected back into the middle of the polymer. Then the crack is confined within the polymer film and vibrates back and forth between the two substrates so as to relieve the largest tensile

stress in its path⁶ (see Fig. 1(c)). The crack front propagating from one edge to the other of the substrate brings out self-assembled grooves parallel to it. Fig. 1(d) demonstrates the schematic of LC molecules mainly aligning parallel to the self-formed grooves.

In our experiments, we found that the wavelength of periodic grooves is around four times the initial thickness of the thin film which is consistent with that of a previously published report.⁷ Our smallest period is 150 nm and this CIG method potentially provides the possibility of reaching a smaller period by reducing

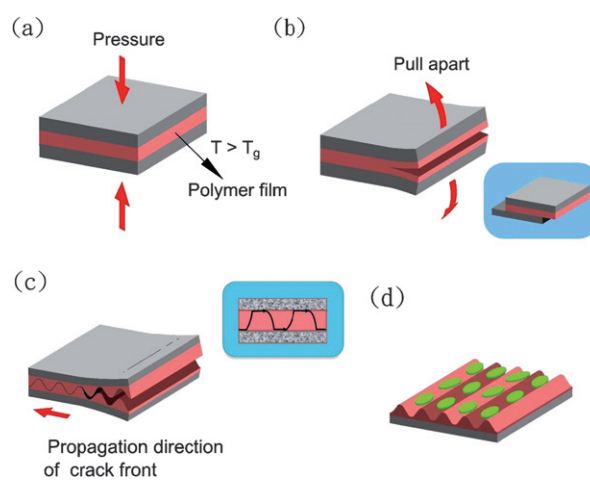


Fig. 1 Schematic of the self-assembled grooves formation using the CIG method. (a) The polymer film is first cast on one substrate and then superimposed on the other bare substrate. Applying pressure and heating above the glass transition temperature (T_g) of the polymer film would enhance adhesion between the polymer film and the substrates. (b) After pressure and heat are applied, the substrates are pulled apart (see inset). Since the substrates are not completely overlapping, this test sample could be separated easily without requiring a razor blade. (c) The separation wavefront vibrates back-and-forth between the upper and bottom substrates to create periodic and complementary grooves on each substrate. The inset shows the cross section of crack front propagating inside the polymer film. (d) Molecules would align principally along the direction of grooves due to the minimization of LC elastic energy.

Department of Physics, National Taiwan University, Taipei, 10617, Taiwan. E-mail: tclin@phys.ntu.edu.tw; cychao@phys.ntu.edu.tw

the film thickness. In this work, the period is tuned for changing anchoring energy to improve the contrast ratio (CR) and the measured opto-electrical curve is comparable to that of traditionally reflective LC cells. Additionally, the anchoring energy of the self-assembled grooves is $\sim 10^{-5} \text{ N m}^{-1}$ which is quite close to the value using PI rubbing. This CIG method generating grooves from a featureless film is low-cost and simple. Moreover, it provides a much more rapid and larger-domain patterning method than E-beam and AFM lithography. Compared to conventional cloth rubbing and AFM scratching, this CIG method inducing self-assembled grooves also circumvents grazing damage, dust contamination and residual static electricity problems. Especially for LC devices with plastic substrates, it performs a much lower processing temperature which is incapable by PI rubbing. The CIG method not only offers an appealing alternative to existing technologies for LC molecules alignment but also promises to be applied to the roll-to-roll process in the future.

2. Experiments and discussions

2.1. Sample preparation

For the CIG method, amorphous polymer consisting of glassy material is essential to the formation of self-assembled grooves. During the cracking, the amorphous polymer, which is non-crystalline and has no-long range molecular order, would create grooves with the same shape across a large area. On the contrary, a polycrystalline material would hamper the formation of self-assembled grooves owing to its anisotropic property. In our experiments, we choose polystyrene (PS, with a molecular weight of $M_w = 1.5 \text{ kg mol}^{-1}$) which is a linear homopolymer dissolved in the toluene solvent (0.5–2% solution by weight). During spin coating, the volatile toluene solvent would evaporate. Baking the substrates a little over the toluene's boiling point ($T_b = 110 \text{ }^\circ\text{C}$) could facilitate removal of the solvent. It deserves to be mentioned that clean substrates and steady casting are required to achieve a flat film in experiments. Because dust or nonuniform polymer thickness would not only cause the wave front to change its propagating direction but also induce different pattern rather than grooves. Fig. 2(a) shows that a nonuniform polymer film

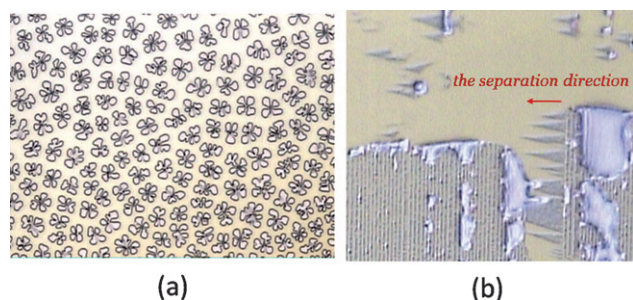


Fig. 2 (a) After being broken up, a nonuniform polymer film would produce flower-like pattern which is similar to the result generated by lithography induced self-assembly (LISA).^{8,9} (b) The apexes of the triangular pattern (see arrows) point the separation direction. Based on experimental observations, the separation direction is perpendicular to the direction of grooves. This result supports the model that the propagating separation wavefront induces self-assembled grooves.

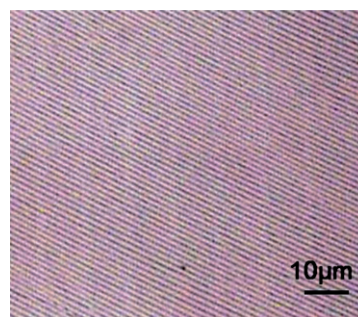


Fig. 3 Optical micrograph of self-assembled grooves with period $\sim 800 \text{ nm}$ from a 200 nm thickness PS film after using the CIG method.

after splitting would result in flower-like pattern, which is similar to the results made by lithography induced self-assembly (LISA).^{8,9} Although it is also a very interesting issue, we still need to focus on the CIG method for LC alignment and avoid the LISA phenomenon in this work. After casting uniform polymer film on a silicon substrate, we overlaid this substrate with the other bare substrate. Apply pressure while heating the whole sandwich structure at temperature $T = 140 \text{ }^\circ\text{C}$ simultaneously. A temperature a little higher than the glass transition temperature of PS ($T_g = 115 \text{ }^\circ\text{C}$) could change the glassy PS film into a rubbery film. Pressing and heating cause polymer film to attach more strongly to the substrate. If the adhesion is not enough, the separation through cracking would occur in the interface between the PS film and silicon surface, not within the PS film, then grooves would not form. Increasing the adhesive force would extend the area of pattern of the grating for several centimeters or even larger. The applied heat and pressure were released after 10 min. The important point is that sample separation must be at the temperature below T_g of polymer. In Fig. 2(b), the small mark of triangular shape represents the direction of the crack which appears if the sample is not cooled down while the separation has occurred. If the separation temperature was higher than T_g , self-assembled grooves would not appear due to the rubbery polymer film, which is easily deformed. In light of the experimental results, we find that the propagating direction is perpendicular to the grooves which is consistent with the earlier results proposed by Chai and Fleck *et al.*^{10,11} After being cooled down to room temperature ($\sim 25 \text{ }^\circ\text{C}$), the PS film becomes brittle and the sample was fractured into two pieces to result in the formation of polymer grooves with the complementary shape on each substrate. Fig. 3 shows the optical micrograph of CIG grating (period $\sim 800 \text{ nm}$) across a large area. In the following, we measure the details of self-assembled grooves by AFM and scanning electron microscope (SEM).

Table 1 The film thickness as a function of the solution concentration (with the same frequency of spin coating).

The concentration of PS toluene solution (by weight)	Film thickness
0.5%	30–40 nm
1%	75–100 nm
1.5%	110–160 nm
2%	175–300 nm

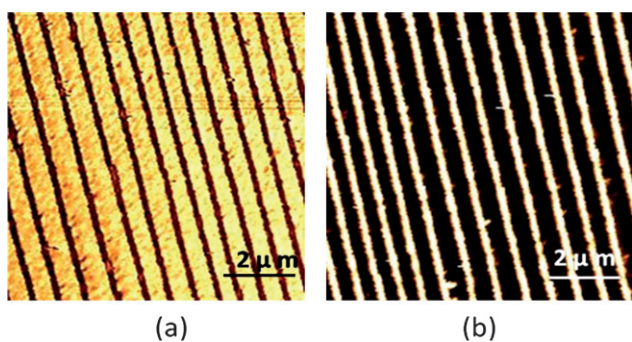


Fig. 4 The two AFM images are surface morphology of polymer grooves from the upper and bottom substrates of the same sample after splitting. The grooves on each substrate are nonsymmetrical but complementary and with the same period (~ 600 nm).

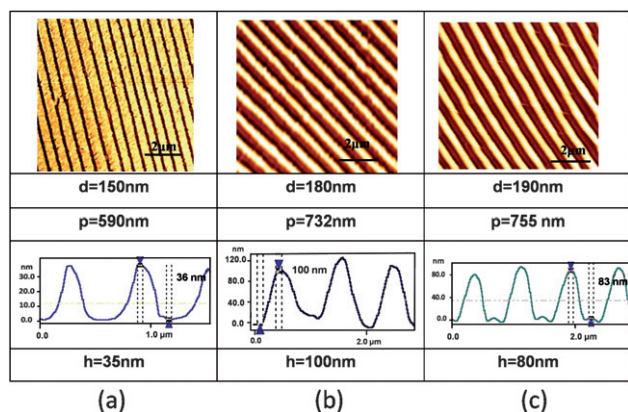


Fig. 5 AFM measurement of the period and height of some self-assembled grooves. (a) The thickness of the polymer film from 1.5% PS toluene solution is ~ 150 nm. The period p of grooves is ~ 600 nm and the height h is ~ 35 nm after splitting. (b) The thickness of the polymer film from 2% PS toluene solution is ~ 180 nm. After splitting, the values of p and h are ~ 732 nm and ~ 100 nm, respectively. (c) The thickness of the polymer film from 2% PS toluene solution is ~ 190 nm. The values of p and h are ~ 755 nm and ~ 80 nm after splitting. Based on numerous experiments, we found that the period is proportional to the film thickness and the height is around one half of film thickness but not necessarily.

2.2 Measurements of self-assembled polymer grooves

Varying the concentration of PS toluene solution from 0.5% to 2% could get different PS film thickness after casting at the fixed frequency. The frequency of spin coating could not be too low, otherwise it would cause a nonuniform polymer film with radial distribution. As shown in Table 1, each concentration corresponds to a respective range of thin film thickness. A more dilute PS solution would result in a thinner film. However, the thinner film takes more attention to control the quality of film uniformity. In our work, the smallest film thickness is 35 nm from 0.5% PS toluene solution. By increasing the concentration of solution to 2%, the film thickness comes up to around 200 nm. Due to the sample arrangement is a little misfit-layered, we could easily split the attached sample apart into two substrates both with polymer grooves on the surfaces. The grooves on bottom and upper silicon substrates are nonsymmetrical, but complementary with the same period. Fig. 4 is the complementary grooves with period ~ 600 nm on the each substrate. The morphology of the PS film was inspected by AFM; the obtained period and height of grooves correspond to each different film thickness (see Fig. 5). With regards to Fig. 5, when the polymer thickness are 150, 180, and 190 nm, the pitch of grooves are about 590, 732, and 755 nm, and the height are 35, 100, and 80 nm respectively. The height is not exactly equal to the film thickness. It depends on the path of the vibrating crack front and is mostly around the half of thickness or even smaller. In this work, we observe that adhesion or annealing temperature would not affect the period of grooves, while it merely determines whether grooves would form or not. We found the period p of self-assembled grooves solely depends on the film thickness d and the period is around four times the thickness which is in consistent with Chou's work.^{7,12} Hence the period could simply vary by adequately tuning the film thickness.

Fig. 6 represents SEM photographs of PS grooves of four different periods. Before taking SEM photographs, sputtering of a gold thin film on the PS surface is needed to prevent PS from melting at a high local energy. From Fig. 6(a) to (c), the period is about 792, 895, 980 nm formed in film thicknesses of 200, 220, 240 nm, respectively. Fig. 6(d) demonstrates a self-assembled groove across a large area ($p \sim 900$ nm). According to the AFM and SEM results, we find the groove period p is a function of film thickness d . Fig. 7 demonstrates the relationship between period

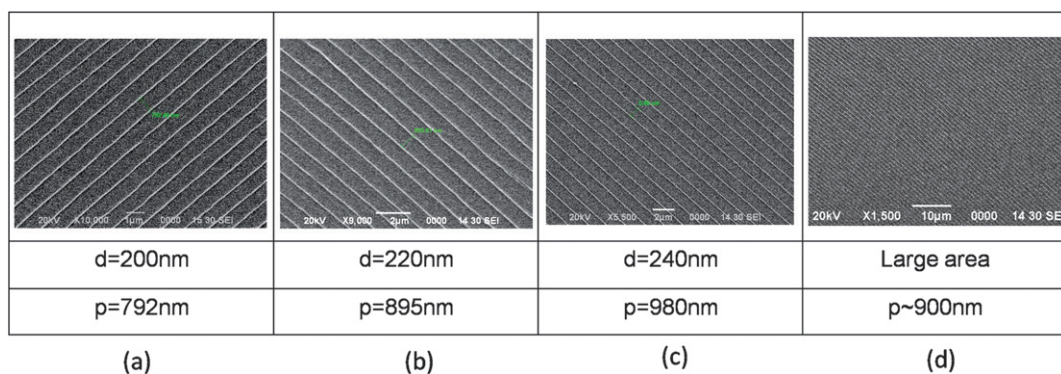


Fig. 6 SEM micrographs of the self-assembled grooves with different periods (PS film is coated with gold film). The polymer films of (a–d) are all from 2% PS toluene solution. The film thicknesses are 200, 220, 240 nm and the period of the grooves are 792, 895, 980 nm, respectively. The groove pattern could be stretched to a very large area as shown in (d).

p and thickness d . By varying the PS concentration as mentioned above, the obtained film thickness ranges from 35 nm to 245 nm. We measured the period p of grooves is from 150 nm to 960 nm. The upper limit of the concentration in our work is 2% which results in a polymer film of about 175–300 nm in thickness. However, for sufficient alignment in LC devices, the period of grooves should be controlled below the LC correlation length ($\sim 1 \mu\text{m}$).¹³

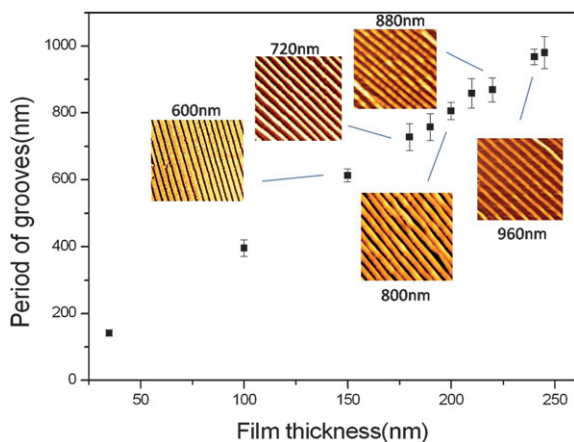


Fig. 7 Period of grooves as a function of polymer film thickness. (The insets are AFM images and the width of each inset is $10 \mu\text{m}$.) By controlling the film thickness from 35 nm to 245 nm, we found the period of grooves could vary from ~ 150 nm to $\sim 1 \mu\text{m}$.

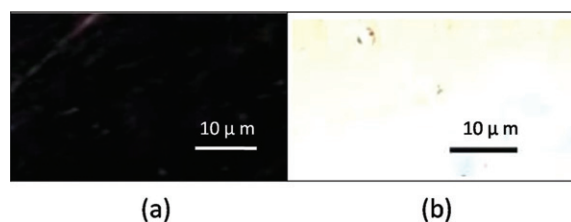


Fig. 8 The crack-induced self-assembled PS grooves are employed to align LC molecules and used to fabricate LC cells as MTN cells. Under polarizing optical microscope, (a) is the normal black state with zero applied voltage and (b) is the bright state with bias voltage about 6 V.

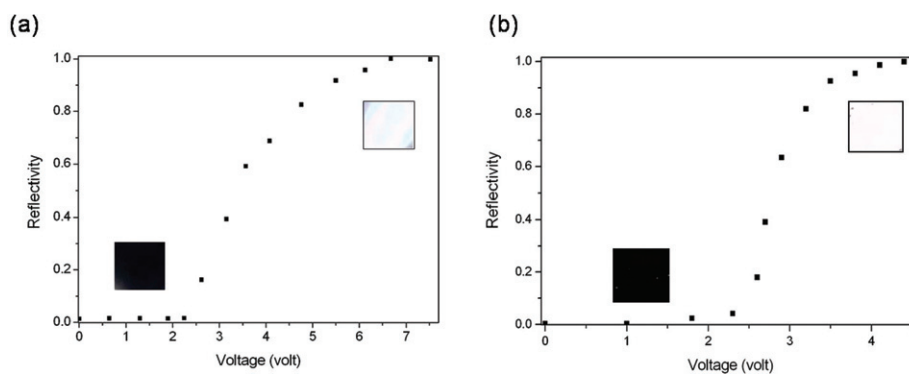


Fig. 9 Reflectivity of MTN cells with different groove periods. (The insets are micrographs under polarizing optical microscope.) (a) The period of grooves is ~ 800 nm and the height is ~ 85 nm. (b) The period of grooves is ~ 600 nm and the height is ~ 100 nm. The calculated anchoring energy of (b) ($W \sim 10^{-5} \text{ N m}^{-1}$) is higher than that of (a) ($W \sim 10^{-6} \text{ N m}^{-1}$) and the contrast ratio of (b) (CR ~ 350) is better than that of (a) (CR ~ 75).

2.3 Fabrication and measurements of liquid crystal cells

We utilized a silicon substrate with crack-induced polymer grooves as the bottom substrate which was then covered by a conventional indium-tin-oxide (ITO) glass coated with PI planar alignment layer as the upper substrate. The direction of crack-induced grooves was set orthogonal to the PI rubbing direction on the opposite substrate. Then, we filled this empty cell with a 4-*n*-pentyl-4'-cyanobiphenyl (5CB) LCs at room temperature and the cell gap is $1.5 \mu\text{m}$. Therefore, the director configuration of LCs sandwiched between the crack-induced groove substrate and rubbed PI layer becomes twisted by 90° . The cells are inspected by a polarizing optical microscope in its reflection mode and the polarizer setting is demanded to obtain maximum darkness with zero voltage for the LC cell (see Fig. 8(a)). Thus, the patterned area (period ~ 800 nm, height ~ 100 nm) of the cell belongs to normal black. The polarizer setting makes the polarizer and the LC director near the upper substrate not parallel but with some angle to form a mixed-mode twisted nematic (MTN) LC cell.¹⁴ In direct-view display, the MTN LC cell requiring only one front polarizer could thus prevent the parallax. The doped and polished silicon substrate patterned by crack-induced self-assembled grooves could thus be simultaneously used for LC alignment, the cell electrode and the mirror reflector. Applying the voltage between the ITO and p-type silicon substrates, the patterned LC cell, *i.e.* normally black mode, started to change its phase retardation and became brighter as shown in Fig. 8(b).

Fig. 9 demonstrates the voltage-dependent light reflectance (RV curve) of the reflective MTN LC cell. Comparing Fig. 9(a) and (b), the threshold voltages of these two RV curves are both around 2.3 V, because the threshold voltage is mainly determined by the LC material.¹⁵ Increasing the applied voltage, the phase retardation came into π resulting in the cell being the bright state. According to Berreman's theory,¹⁶ the anchoring energy resulted from grooves is $W = 2\pi^3 K A^2 / \lambda^3$, which A is the amplitude, λ is the period of groove, and K is the Frank elastic constant of the LC ($K_{5CB} = 2 \times 10^{-12} \text{ N}$). For a MTN LC cell in Fig. 9(a), with $\lambda \sim 800$ nm and $A \sim 100$ nm, the anchoring energy W is $\sim 2.4 \times 10^{-6} \text{ N m}^{-1}$. For the other MTN cell in Fig. 9(b), with $\lambda \sim 600$ nm and $A \sim 85$ nm, the anchoring energy W is $\sim 4.1 \times 10^{-6} \text{ N m}^{-1}$ which is ~ 1.7 times that in Fig. 9(a).

The larger anchoring energy mooring LC molecules more strongly should improve the dark state and thus achieve a higher contrast ratio (CR) in LC device. In our experiments, we found that the CR of the MTN LC cell in Fig. 9(b) is about 350, which is five times larger than that in Fig. 9(a) (CR only ~ 75), and this result coincides with the calculated anchoring energy.

Nowadays, the anchoring energy of conventional PI rubbing is 10^{-4} – 10^{-5} N m $^{-1}$ and for AFM rubbing is $\sim 10^{-6}$ N m $^{-1}$.^{17,18} As already stated, the anchoring energy of crack-induced polymer grooves is $\sim 10^{-5}$ N m $^{-1}$, which is an order of magnitude between PI and AFM rubbing. This anchoring energy of the PS self-assembled grooves is enough to give a good control of LC molecules.

3. Conclusions

We utilize an express and high-throughput method for LC alignment. More than successfully aligning LCs, the CIG method generates self-assembled grooves also enables alignment of other molecules, such as dyes and biomolecules, for optoelectronic devices and cell adhesion applications, *etc.*^{19,20} In our experiment, the measured period of the grooves is found to be proportional to the film thickness. Thus, the period could be tuned as required *via* changing the film thickness. The anchoring energy of the crack-induced grooves approaches that of conventional PI rubbing. This cutting edge method is low cost, has a low process temperature, has no dust contamination, no residual static electricity, and holds the promise of patterning self-formation grooves on glass or plastic substrates for LCD applications. It provides an alternative comparable to the existing mainstream

LCD technologies and enables application to roll-to-roll processes in the future.

Notes and references

- 1 F. C. Frank, *Discuss. Faraday Soc.*, 1958, **25**, 19.
- 2 D. M. Tennant, T. L. Koch, P. P. Mulgrew, R. P. Gnall, F. Ostermeyer and J. -M. Verdiell, *J. Vac. Sci. Technol., B*, 1992, **10**, 2530.
- 3 J. H. Kim, M. Yoneya and H. Yokoyama, *Nature*, 2002, **420**, 159.
- 4 S. Y. Chou, P. R. Krauss and P. J. Renstrom, *Science*, 1996, **272**, 85.
- 5 K. O. Hill, B. Malo, F. Bilodeau, D. C. Jackson and J. Albert, *Appl. Phys. Lett.*, 1993, **62**, 1035.
- 6 B. Freund, *Nat. Nanotechnol.*, 2007, **2**, 537.
- 7 L. F. Pease III, P. Deshpande, Y. Wang, W. B. Russel and S. Y. Chou, *Nat. Nanotechnol.*, 2007, **2**, 545.
- 8 S. Y. Chou and L. Zhuang, *J. Vac. Sci. Technol.*, 1999, **17**, 3197.
- 9 J. Peng, Y. Han, Y. Yang and B. Li, *Polymer*, 2003, **44**, 2379.
- 10 H. Chai, *Int. J. Fracture*, 1986, **32**, 211.
- 11 N. A. Fleck, J. W. Hutchinson and Z. Suo, *Int. J. Solids Structures*, 1991, **27**, 1683.
- 12 P. A. Deshpande, PhD Dissertation Princeton University, 2005.
- 13 A. Rastegar, M. Skarabot, B. Blij and Th. Rasing, *J. Appl. Phys.*, 2001, **89**, 960.
- 14 S. T. Wu, D. K. Yang, *Reflective Liquid Crystal Displays*, ed. A. C. Lowe, Wiley-SID, UK 2001, p. 89–108.
- 15 X. Nie, R. Lu, H. Xianyu, T. X. Wu and S. T. Wu, *J. Appl. Phys.*, 2007, **101**, 103110.
- 16 D. W. Berreman, *Phys. Rev. Lett.*, 1972, **28**, 1683.
- 17 H. Yokoyama, *Mol. Cryst. Liq. Cryst.*, 1988, **165**, 265.
- 18 J. H. Kim, M. Yoneya, J. Yamamoto and H. Yokoyama, *Nanotechnology*, 2002, **13**, 133.
- 19 P. L. Burn, A. B. Holmes, A. Kraft, D. D. C. Bradley, A. R. Brown, R. H. Friend and R. W. Gymer, *Nature*, 1992, **356**, 47.
- 20 M. Arnold, E. A. Cavalcanti-Adam, R. Glass, J. Blümmel, W. Eck, M. Kantlehner, H. Kessler and J. P. Spatz, *ChemPhysChem*, 2004, **5**, 383.